

# Compact Optical Add-Drop Multiplexers With Parent-Sub Ring Resonators on SOI Substrates

Hai Yan, Xue Feng, Dengke Zhang, Kaiyu Cui, Fang Liu, and Yidong Huang

**Abstract**—A four-channel integrated optical add/drop multiplexer is experimentally demonstrated on a silicon-on-insulator substrate. With the help of a parent-sub microring resonator structure, compact footprint, large free spectral range, and uniform channel spacing are achieved simultaneously. Through controlling the resonance matching between the parent and sub-rings through thermo-optic effect, each channel can be switched independently between the states of dropping and passing through. The thermal tuning efficiency is as high as 0.27 nm/mW. Typically, for dropping state, all four channels can be de-multiplexed to the drop ports with 2 dB drop loss, 18 dB through port extinction, and less than  $-20$  dB channel crosstalk.

**Index Terms**—Integrated optics, optical resonators, silicon, wavelength division multiplexing.

## I. INTRODUCTION

SILICON microring resonator enables new technology in integrated photonic devices, including switches, spectral filters, optical delay lines, modulators, and biosensors owing to its ultra-compact size, high quality factor, and compatibility with complementary metal-oxide-semiconductor (CMOS) technology [1]. Side-coupled with bus waveguides, microring resonator can be readily used as an add/drop filter and cascaded to constitute optical add/drop multiplexer (OADM) for wavelength division multiplexing (WDM) systems. OADM has been widely used in fiber-optic communications and is likely to find its role in short distance optical networks including on-chip interconnects in the future. In previous reports, the performance of single-channel microring add/drop filter has been improved significantly. The free spectral range (FSR) can be extended to more than 30 nm using ultra-small ring resonator [2], [3] or coupled rings with different radii (Vernier effect) [4], [5]. Box-like passband is also achieved by high-order coupled ring resonator filter [6], [7]. On the other hand, multiple-channel OADMs have also been demonstrated by cascading add/drop filters in an array [8]–[11]. The wavelength shift between adjacent channels can be realized by varying the

Manuscript received April 7, 2013; revised May 14, 2013 and May 29, 2013; accepted June 4, 2013. Date of publication June 11, 2013; date of current version July 12, 2013. This work was supported in part by the National Basic Research Program of China under Grants 2011CBA00608 and 2011CBA00303, and in part by the National Natural Science Foundation of China under Grants 61036011 and 61036010.

The authors are with the Department of Electronic Engineering, Tsinghua National Laboratory for Information Science and Technology, Tsinghua University, Beijing 100084, China (e-mail: h-yan10@mails.tsinghua.edu.cn; x-feng@tsinghua.edu.cn; zdk08@mails.tsinghua.edu.cn; kaiyucui@tsinghua.edu.cn; liu\_fang@tsinghua.edu.cn; yidonghuang@tsinghua.edu.cn).

Color versions of one or more of the figures in this letter are available online at <http://ieeexplore.ieee.org>.

Digital Object Identifier 10.1109/LPT.2013.2267232

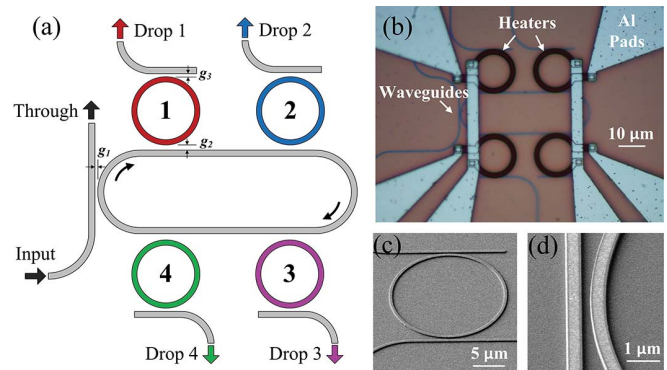


Fig. 1. (a) Four-channel OADM with parent-sub microring structure; (b) microscope image of the fabricated OADM with micro-heaters on each of the sub-rings; (c) and (d) scanning electron microscope (SEM) images of a microring resonator and waveguides.

perimeters of ring resonators [8] or thermal tuning [9]–[11]. The former approach relies on high-resolution electron beam lithography (EBL) to obtain uniform channel spacing, which is not cost-effective for high-volume manufacturing. The latter one reduces the requirement on fabrication, but a large number of heaters are required if high-order coupled ring resonators are adopted for each channel.

To deal with the problems mentioned above, we have proposed a parent-sub microring structure [12], which has the potential to achieve large FSR, compact size, uniform channel spacing, and second-order filter response at the same time. In this letter, a 4-channel OADM with parent-sub microring structure is experimentally demonstrated. The device is fabricated with CMOS-compatible technology and characterized by measuring the spectra of all output ports. The output spectra show that all four channels can be de-multiplexed to the drop ports with 2 dB drop loss, 18 dB through port suppression, and less than  $-20$  dB channel crosstalk. By thermally controlling the resonance matching between parent and sub-rings, each channel can be switched independently between the states of dropping and passing through.

## II. PRINCIPLE, DESIGN, AND FABRICATION

Fig. 1(a) is the layout of our proposed 4-channel OADM. There are four sub-rings coupled to a parent ring. The parent ring's resonance wavelengths are considered to be coincident with the center wavelengths of input WDM channels. The resonance wavelengths of the four sub-rings are different from each other and when they are aligned to the four WDM channels separately, light signal of each channel would go through the parent ring and one of the sub-rings before

reaching the corresponding drop port. When the resonances of sub-ring do not match the channel wavelengths, the signals would be blocked by sub-rings and propagate to the through port directly. With thermal tuning of the sub-rings, the resonances could be shifted so that the corresponding signals could be controlled to output from either the drop ports or the through port. Such parent-sub microring structure helps make device footprint more compact comparing to the usual arrangement of cascading microring add/drop filters in an array [8]–[11]. Furthermore, since coupled ring resonators with different perimeters ( $L_1$  and  $L_2$ , supposing  $L_1/L_2 = m_1/m_2$ ,  $m_1$  and  $m_2$  are co-prime integers) are adopted, FSR would be extended to  $m_1 \cdot FSR_1$  (or  $m_2 \cdot FSR_2$ ) due to Vernier effect [4], [5]. Moreover, the center wavelengths of the channels are determined by the resonances of a single ring (the parent ring) so that the channel spacing is naturally uniform in a wide wavelength range. The detailed operating principle could be found in our previous report [12].

Here, the wavelengths of the WDM signals are assumed to be around 1550 nm with 4.8 nm channel spacing. The waveguides in the device are all silicon rib waveguides with a width of 450 nm, a height of 220 nm, and a slab layer thickness of 60 nm. The estimated group refractive index is 3.76 for fundamental transverse electric (TE) mode. The FSR of the parent ring is designed equal to the channel spacing (4.8 nm) and the FSR of the sub-rings is set to 12 nm (2.5 times of 4.8 nm). Then the FSR of the coupled rings should be 24 nm due to Vernier effect. This value could be further expanded by adjusting the FSR ratio between parent and sub-rings. The perimeters of the microrings can thus be determined:  $L_1 = 133 \mu\text{m}$  for the parent ring,  $L_2 = 53.2 \mu\text{m}$  for the sub-rings. A racetrack shape is adopted for the parent ring to reduce the footprint and facilitate the alignment of the sub-rings. The gap distance between the bus waveguide and the parent ring ( $g_1$ ), the parent ring and sub-rings ( $g_2$ ), sub-rings and waveguides ( $g_3$ ) are carefully designed as  $g_1 = 200 \text{ nm}$ ,  $g_2 = 425 \text{ nm}$ , and  $g_3 = 200 \text{ nm}$ , respectively, concerning the bandwidth and flatness of passband as well as channel crosstalk following the discussions in [12]. The corresponding amplitude coupling coefficients are estimated to be  $t_1 = 0.36$ ,  $t_2 = 0.067$ ,  $t_3 = 0.35$ , respectively. At the end of the input and output waveguides, an inverse waveguide taper is used to couple with optical fibers.

The device is fabricated on a silicon-on-insulator (SOI) wafer through the photonics prototyping service at the Institute of Microelectronics in Singapore. The thickness of the top silicon layer and buried oxide layer is 220 nm and  $2 \mu\text{m}$ , respectively. A 248 nm deep UV lithography is used to define the pattern. Then the waveguides are etched with inductively coupled plasma (ICP) reactive ion etch (RIE) (Fig. 1(c) and (d)). After depositing  $\text{SiO}_2$  cladding on the silicon waveguides, TiN heater is formed on the cladding over the sub-rings to thermally tune their resonances separately. The heaters are  $2 \mu\text{m}$  wide and connect to the Al pads above (Fig. 1(b)).

### III. MEASUREMENTS AND RESULTS

A tunable laser source is used to characterize the output power spectrum of the fabricated OADM sample. The output

light from the tunable laser is rotated by a polarization controller to excite fundamental TE mode in the silicon rib waveguide. Single-mode lensed tapered fibers are mounted on a computer-controlled alignment stage to couple light in and out of the device. We scan the input wavelengths at 0.05 nm per step and record the output optical power to obtain the spectrum.

Fig. 2 (a) shows the measured power spectra of all output ports without thermal tuning. The four dips (at 1538.55 nm, 1542.90 nm, 1547.35 nm, and 1551.80 nm) in the through port response (black line in Fig. 2 (a)) represents the resonances of the parent ring, *i.e.*, the four WDM channels. The spacing for adjacent channels is uniform and the value is 4.45 nm. In each drop port response, there are peaks at resonance wavelengths of both the parent and sub-ring. For example, in the spectrum of drop-port 2 (green line in Fig. 2 (a)), apart from the four peaks at the same wavelength with the four dips in the through port, there are two peaks at 1543.45 nm and 1554.45 nm. They correspond to the resonances of sub-ring 2 (FSR = 11.00 nm). The resonances of the microring resonators are randomly distributed since they are highly sensitive to the fabrication error.

With proper thermal tuning of all four sub-rings, the corresponding resonances could be aligned to the channel wavelengths, as shown in Fig. 2(b). In each drop port response, there is one major peak within one of the four channels, while in the through port spectrum there appears four deep notches. It reveals that the WDM signals are directed to different drop ports. In the zoom-in view of Fig. 2(b), the 3-dB bandwidth is 0.15 nm with a drop loss of 2 dB and a shape factor (1dB-10dB bandwidth ratio) of 0.4. The through port extinction is about 18 dB and the channel crosstalk is less than  $-20 \text{ dB}$ . The passband top is nearly flat but has a slope due to a tiny misalignment between the resonance of parent and sub- microring. This verifies the optimum coupling coefficients relation for maximally flat passband in our previous paper [12]. The optimum relation is applicable for this 4-channel parent-sub microring structure, although it is deduced from single-channel coupled-microring filter. This is probably because light signals of different channels pass the parent ring and their own sub-rings without affecting each other significantly. Therefore, the impact of coupling coefficients on the passband performance can be independently considered for each channel.

Furthermore, each sub-ring could be switched between the operating states of dropping and passing through. Two typical cases are presented in Fig. 2(c) and (d). In Fig. 2(c), the signal in Channel 3 is switched to pass the through port with  $\sim 3 \text{ dB}$  additional loss and other channels are nearly unaffected. In Fig. 2(d), all channels pass through the device with 2–4 dB additional loss and the crosstalk to the drop ports is less than  $-15 \text{ dB}$ .

The electrical properties of the micro-heaters are also experimentally analyzed. The measured resistance of all four heaters are  $220 \pm 5 \Omega$ . The measured curve shows a linear relationship between the resonance wavelength shift and the applied electric power with a slope of 0.27 nm/mW (black line in Fig. 3). A slight resonance shift in the parent ring

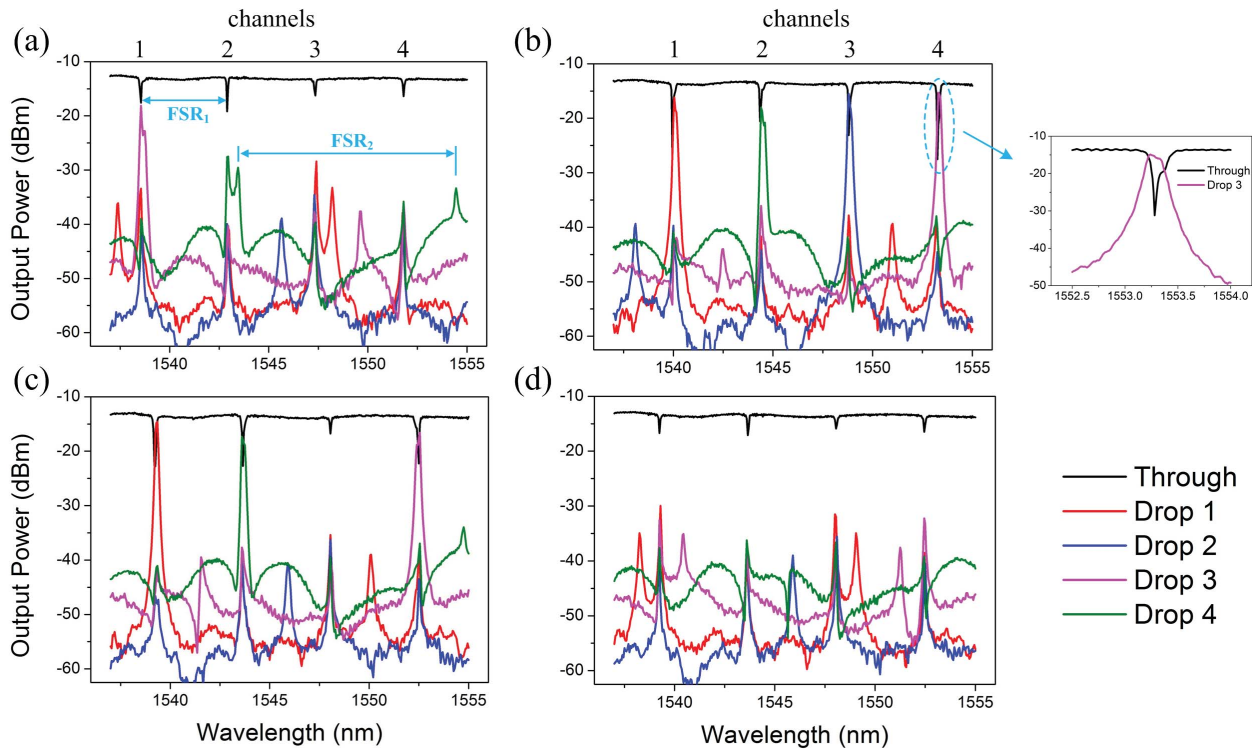


Fig. 2. Measured output power spectra under different tuning conditions (a) no tuning power is applied, (b) the resonances of sub-rings are tuned to match the four channels, respectively, (c) only Channel 3 is tuned to the through port, and (d) all channels are tuned to output from the through port.

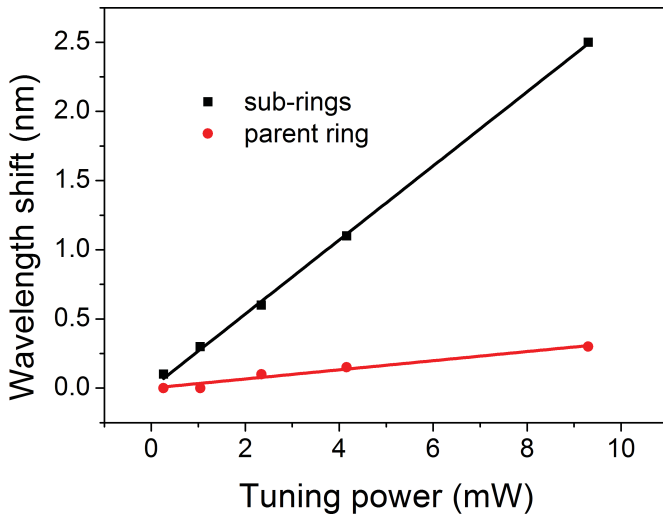


Fig. 3. Thermal tuning power versus corresponding resonance wavelength shift of parent- and sub-rings.

is also observed (0.03 nm/mW, red line in Fig. 3), which is probably due to the thermal crosstalk between the sub- and parent microrings. The crosstalk should be suppressed to avoid the parent-ring resonances' deviation from given channels. Possible solutions include moving heaters away from the parent ring and adding thermal isolation trenches around the heaters [13].

#### IV. DISCUSSION

When the WDM signals are switched to the through port by shifting the sub-microring resonance away from the parent ring

TABLE I  
POWER CONSUMPTION FOR SUB-RINGS

FIG NO.	SUB-RING 1 (mW)	SUB-RING 2 (mW)	SUB-RING 3 (mW)	SUB-RING 4 (mW)
FIG. 2(B)	9.1	10.6	13.3	2.4
FIG. 2(C)	6.8	0	10.8	0
FIG. 2(D)	3.7	0	5.3	6.0

resonance (see Fig. 2(c) and (d)), there is 2-4 dB throughput transmission loss due to parent ring resonance dip, which is undesired for practical applications. Actually, such loss could be further reduced. Because the parent ring is over-coupled to the bus waveguide (estimated self-coupling coefficient  $r_1 = 0.93 < \text{round-trip transmission } a = 0.99$ ), the resonance dip can be reduced by strengthening the over-coupling. There are two methods to achieve it. One is to reduce  $r_1$  so that the coupling between the waveguide and the parent ring can be strengthened. The other is to lower the propagation loss in the microring. If the former measure is adopted,  $r_3$  should be increased to maintain the optimum relation between the coupling coefficients that guarantees flat-top drop port response.

The power consumption for thermal tuning of the sub-rings in Fig. 2(b), (c) and (d) is listed in Table I. It is mainly determined by the resonance misalignment between the parent and sub- microrings, which is very sensitive to fabrication errors. So the power consumption is not very predictable. Additionally, the red-shift in parent ring resonance due to the

thermal crosstalk further increases the tuning power needed for the sub-rings. However, the situation can be improved by enhancing the heater efficiency and minimizing the thermal crosstalk. In a recent report [11], the heater efficiency in thermally controlled WDM filters has been improved by an order of magnitude using free-standing microring structure. Thermal crosstalk can be suppressed, as mentioned in Section III, by putting the heater far enough away from the parent ring and adding thermal isolation trenches around heaters [13].

Combining our numerical simulations [12] with the experiment results here, some key steps in designing the OADM with parent-sub microring resonators can also be summarized. First, the FSR of the parent ring is determined according to channel spacing. The FSR of the sub-ring should be wider and should not coincide with two or more channels at the same time. Then, the perimeters of the microrings can be decided. Second, the coupling coefficient between parent and sub-microrings ( $t_2$  or  $r_2$ ) should be first chosen because the 3dB bandwidth of passband is mainly determined by it. Then, other coupling coefficients ( $t_1$ ,  $r_1$  and  $t_3$ ,  $r_3$ ) could be calculated following the optimum relation among coupling coefficients [12]. It should be mentioned that  $r_1$  could be properly settled to a lower value so that the throughput transmission loss could be further reduced when the channels are switched to through port. After all the coupling coefficients are obtained, the gap distances can be estimated.

## V. CONCLUSION

In this letter, a 4-channel integrated optical add/drop multiplexer with parent-sub microring resonator structure is experimentally demonstrated on a SOI substrate. Extended FSR without introducing significant bending loss, nearly uniform channel spacing, second-order filter response, and compact footprint suitable for high-density integration are achieved in fabricated devices. With thermal tuning of the sub-rings, we show that the device is able to work as a de-multiplexer. Furthermore, each of the channel's operating state could be independently switched. Wider FSR and better filter response are expected by optimizing resonator perimeters and coupling coefficients.

## ACKNOWLEDGMENT

The authors would like to acknowledge Dr. W. Zhang for valuable discussions and helpful comments. The authors also thank the Institute of Microelectronics, Singapore for device fabrication.

## REFERENCES

- [1] W. Bogaerts, *et al.*, "Silicon microring resonators," *Laser Photon. Rev.*, vol. 6, pp. 47–73, Jan. 2012.
- [2] A. M. Prabhu, A. Tsay, Z. Han, and V. Van, "Ultracompact SOI microring add-drop filter with wide bandwidth and wide FSR," *IEEE Photon. Technol. Lett.*, vol. 21, no. 10, pp. 651–653, May 15, 2009.
- [3] S. Xiao, M. H. Khan, H. Shen, and M. Qi, "Silicon-on-insulator microring add-drop filters with free spectral ranges over 30 nm," *J. Lightw. Technol.*, vol. 26, no. 2, pp. 228–236, Jan. 15, 2008.
- [4] R. Boeck, N. A. F. Jaeger, N. Rouger, and L. Chrostowski, "Series-coupled silicon racetrack resonators and the Vernier effect: Theory and measurement," *Opt. Express*, vol. 18, pp. 25151–25157, Nov. 2010.
- [5] W. S. Fegadolli, *et al.*, "Reconfigurable silicon thermo-optical ring resonator switch based on Vernier effect control," *Opt. Express*, vol. 20, no. 13, pp. 14722–14733, 2012.
- [6] F. Xia, M. Rooks, L. Sekaric, and Y. Vlasov, "Ultra-compact high order ring resonator filters using submicron silicon photonic wires for on-chip optical interconnects," *Opt. Express*, vol. 15, pp. 11934–11941, Sep. 2007.
- [7] S. Xiao, M. H. Khan, H. Shen, and M. Qi, "A highly compact third-order silicon microring add-drop filter with a very large free spectral range, a flat passband and a low delay dispersion," *Opt. Express*, vol. 15, pp. 14765–14771, Oct. 2007.
- [8] S. Xiao, M. H. Khan, H. Shen, and M. Qi, "Multiple-channel silicon micro-resonator based filters for WDM applications," *Opt. Express*, vol. 15, pp. 7489–7498, Jun. 2007.
- [9] X. Zheng, *et al.*, "A tunable 1×4 silicon CMOS photonic wavelength multiplexer/demultiplexer for dense optical interconnects," *Opt. Express*, vol. 18, pp. 5151–5160, Mar. 2010.
- [10] M. Geng, *et al.*, "Four-channel reconfigurable optical add-drop multiplexer based on photonic wire waveguide," *Opt. Express*, vol. 17, pp. 5502–5516, Mar. 2009.
- [11] P. Dong, *et al.*, "1×4 reconfigurable demultiplexing filter based on free-standing silicon racetrack resonators," *Opt. Express*, vol. 18, pp. 24504–24509, Nov. 2010.
- [12] H. Yan, X. Feng, D. Zhang, and Y. Huang, "Integrated optical add-drop multiplexer based on a compact parent-sub microring-resonator structure," *Opt. Commun.*, vol. 289, pp. 53–59, Feb. 2013.
- [13] P. Dong, *et al.*, "Low power and compact reconfigurable multiplexing devices based on silicon microring resonators," *Opt. Express*, vol. 18, pp. 9852–9858, May 2010.